Trajectory Generation for Autonomous Vehicles

Vu Trieu Minh

Tallinn University of Technology, Department of Mechatronics, 19086 Tallinn, Estonia
trieu.vu@ttu.ee

Abstract. This paper presents the problem of trajectory generation for autonomous vehicles with three different techniques in flatness, polynomial and symmetric polynomial equations subject to constraints. Kinematic model for each technique is built subject to constraints including position, body angle, steer angle and their velocities. Simulations for each technique are conducted and compared. Findings in this paper can be used to develop a real-time controller for auto-driving and auto-parking systems.

1 Introduction

This paper studies problem related to trajectory generation for autonomous vehicles moving from a start point to any destination point subject to constraints. Study of this paper can be used to develop a real-time control system for autonomous ground vehicles which can track exactly on any feasible paths from the global positioning system (GPS) maps or/and from unmanned aerial vehicle (UAV) images. This system can be also applied to autonomous unmanned ground vehicles (on road or off road), and auto-parking, auto-driving systems.

Basic studies on the flatness, nonholonomic, and nonlinear systems can be read from the book of Levine J. in [1] where the fundamental motion planning of a vehicle is presented. The flatness and controllability conditions for this nonlinear system are also well investigated and defined. Parking simulation of a two-trailer vehicle is also demonstrated but without the constraint of steer angle and steer angular velocity.

The problem of trajectory generation for nonholonomic system is also presented by Dong W and Guo Y in [2] where two trajectory generation methods are proposed. The control inputs are the second order polynomial equations. By integrating those control inputs, coefficients for those second order polynomial equations are found. However this paper is lacking constraint analysis on the vehicle velocity and the steer angle.

Optimal control based on cell mapping techniques for a car-like robot is studied by Gomez, M. in [3] subject to the energy-optimal constraint and based on bang-bang control theory. This paper shows a simulation of a wheeled mobile robot moving on a path with the steering angle velocity control. However the paper does not mention on the algorithms for generating the vehicle trajectory. Several other

T. Březina and R. Jabloński (eds.), *Mechatronics 2013*,
DOI: 10.1007/978-3-319-02294-9_78,

research papers on optimal trajectories and control of autonomous vehicles can be read in [4], [5], [6], and [7], however most of those studies are based on the real traffic flow roads and the control algorithms are to perform the maneuver tasks such as lane-changing, merging, distance-keeping, velocity-keeping, stopping, and collision avoidance, etc.

This paper, therefore, focuses on the applicable algorithms to generate feasible trajectories from a start point to any destination point subject to vehicle constraints. This paper is the continuation of the previous paper on vehicle sideslip model and estimation by Minh V in [8]. The nonlinear computational schemes for the nonlinear systems are referred to in Minh V and Nitin A. in [9] and [10]. The outline of this paper is as follows: Section 2 describes the kinematic model; Section 3 presents the flatness method; Section 4 presents the polynomial method; Section 5 introduces the symmetric polynomial method and the performance of the three methods; finally, conclusion is drawn in section 6.

2 Kinematic Model of a Vehicle

A kinematic model of a vehicle can be drawn in figure 1:

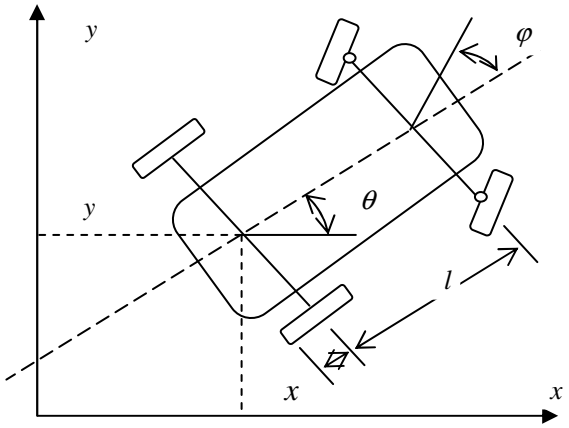

Fig. 1 A simplified vehicle model

The kinematic model of a forward rear-wheel driving vehicle can be written as:

$$\begin{bmatrix} \dot{x} \\ \dot{y} \\ \dot{\theta} \\ \dot{\varphi} \end{bmatrix} = \begin{bmatrix} \cos\theta \\ \sin\theta \\ \dfrac{\tan\varphi}{l} \\ 0 \end{bmatrix} rv_1 + \begin{bmatrix} 0 \\ 0 \\ 0 \\ 1 \end{bmatrix} v_2 \tag{1}$$

where $X = [x, y, \theta, \varphi]'$ is the system state variables, (x , y) are the Cartesian coordinates of the middle point of the rear wheel axis, θ is the angle of the vehicle

body to the *x*-axis, φ is the steering angle, l is the vehicle wheel base, r is the wheel radius, v_1 is the angular velocity of the rear wheel, and v_2 is the angular steering velocity. Given the initial state $X(0)=[x_0, y_0, \theta_0, \varphi_0]'$ at time $t=0$ and the final state $X(T)=[x_T, y_T, \theta_T, \varphi_T]'$ at time $t=T$, the paper generates a feasible trajectory for this vehicle.

Similarly, the model for a forward front-wheel driving vehicle is presented as:

$$\begin{bmatrix} \dot{x} \\ \dot{y} \\ \dot{\theta} \\ \dot{\varphi} \end{bmatrix} = \begin{bmatrix} \cos\theta\cos\varphi \\ \sin\theta\cos\varphi \\ \dfrac{\tan\varphi}{l} \\ 0 \end{bmatrix} rv_1 + \begin{bmatrix} 0 \\ 0 \\ 0 \\ 1 \end{bmatrix} v_2 \tag{2}$$

For a vehicle moving in a reverse direction (backing), the velocity, v_1, of this vehicle is assigned in a minus value:

$$\begin{bmatrix} \dot{x} \\ \dot{y} \\ \dot{\theta} \\ \dot{\varphi} \end{bmatrix} = -\begin{bmatrix} \cos\theta \\ \sin\theta \\ \dfrac{\tan\varphi}{l} \\ 0 \end{bmatrix} rv_1 + \begin{bmatrix} 0 \\ 0 \\ 0 \\ 1 \end{bmatrix} v_2 \tag{3}$$

From the above kinematic models, flatness equations for the vehicle trajectory generation are presented in the next section.

3 Vehicle Flatness Trajectory Generations

From figure 1, the vehicle angular velocity can be calculated as:

$$v_1 = \frac{\sqrt{\dot{x}^2 + \dot{y}^2}}{r} \tag{4}$$

Transformation from equation (1), the vehicle body angle is:

$$\theta = \arctan\left(\frac{\dot{y}}{\dot{x}}\right) \tag{5}$$

From the derivative of the above trigonometric, θ, the body angular velocity, $\dot{\theta}$, is achieved:

$$\dot{\theta} = \frac{\ddot{y}\dot{x} - \ddot{x}\dot{y}}{\dot{x}^2} \frac{1}{\left(\dfrac{\dot{y}}{\dot{x}}\right)^2 + 1} = \frac{\ddot{y}\dot{x} - \ddot{x}\dot{y}}{\dot{x}^2 + \dot{y}^2} = \frac{\tan\varphi}{l} rv_1 \tag{6}$$

Therefore, θ and φ can be directly calculated from variables: $\dot{x}$, $\ddot{x}$, and $\dot{y}$, $\ddot{y}$. And it means that the above system is flat [1]. Thus, all state and input variables can be presented by the flat outputs *x* and *y*.

The boundary conditions for the outputs *x* and *y* are:

$$\frac{\partial^2 y}{\partial x^2} = \frac{\tan\varphi}{l\cos^3\theta} \tag{7}$$

The initial state at time, $t = 0$, to the final state at time, $t = T$ for $x(t)$:

$$x(0) = x_0, \text{ and } x(T) = x_T \tag{8}$$

The initial state for $y(t) = y(0)$ and the final state for $y(t) = y(T)$:

$$y(0) = y_0 = \tan\theta_0 \Rightarrow \frac{\partial^2 y}{\partial x^2}\Big|_{t=0} = \frac{\tan\varphi_0}{l\cos^3\theta_0} \tag{9}$$

$$y(T) = y_T = \tan\theta_T \Rightarrow \frac{\partial^2 y}{\partial x^2}\Big|_{t=T} = \frac{\tan\varphi_T}{l\cos^3\theta_T} \tag{10}$$

From the initial state $(x_0, y_0, \theta_0, \varphi_0)$ at the time $t = 0$ to the final state $(x_T, y_T, \theta_T, \varphi_T)$, under a real condition that $|\dot{x}(t)| \geq \varepsilon > 0$. If it is assumed that, $\varepsilon = \frac{|x_T - x_0|}{2T} > 0$, the trajectory of $x(t)$ can be written freely as:

$$x(t) = \left(\frac{T-t}{T}\right)x_0 + \frac{t}{T}x_T + |x_T - x_0|\frac{t(t-T)}{2T^2} \tag{11}$$

And the trajectory of $y(t)$ can be selected as:

$$y(t) = y_0 + t\alpha_1\tan\theta_0 + t^2\frac{\alpha_2\tan\varphi_0}{2l\cos^3\theta_0} + t^3b_1 + t^4b_2 + t^5b_3 \tag{12}$$

where $\alpha_1 = \frac{2(x_T - x_0) - |x_T - x_0|}{2T}$, $\alpha_2 = \frac{|x_T - x_0|}{T^2}$, and $\alpha_3 = \frac{2(x_T - x_0) + |x_T - x_0|}{2T}$;

and $b = [b_1, b_2, b_3]^* = A^{-1}c$ with $A = \begin{bmatrix} T^3 & T^4 & T^5 \\ 3T^2 & 4T^3 & 5T^4 \\ 6T & 12T^2 & 20T^3 \end{bmatrix}$ and

$$c = \begin{bmatrix} y_T - y_0 - T\alpha_1\tan\theta_0 - T^2\dfrac{\alpha_2\tan\varphi_0}{2l\cos^3\theta_0} \\ \alpha_3\tan\theta_T - \alpha_1\tan\theta_0 - T\dfrac{\alpha_2\tan\varphi_0}{l\cos^3\theta_0} \\ \dfrac{\alpha_2\tan\varphi_T}{l\cos^3\theta_T} - \dfrac{\alpha_2\tan\varphi_0}{l\cos^3\theta_0} \end{bmatrix}.$$

From equation (10),

$$\theta = \arctan\left(\frac{2T^2\left(\alpha_1 \tan\theta_0 + \frac{\alpha_2 \tan\varphi_0}{l\cos^3\theta_0}t + 3b_1t^2 + 4b_2t^3 + 5b_3t^4\right)}{\left(2T(x_T - x_0) - T\left|x_T - x_0\right| + 2\left|x_T - x_0\right|t\right)}\right) \tag{13}$$

and from equation (5),

$$\varphi = \arctan\left(\frac{\left(\frac{\alpha_2 \tan\varphi_0}{l\cos^3\theta_0} + 6b_1t + 12b_2t^2 + 20b_3t^3\right)\left(2T^2\right)^2 l\cos^3\theta}{\left(2T(x_T - x_0) - T\left|x_T - x_0\right| + 2\left|x_T - x_0\right|t\right)^2}\right) \tag{14}$$

The angular velocity of the vehicle in equation (1) can be calculated from (13) and (14).

$$\dot{y}(t) = \left(\alpha_1 \tan\theta_0 + \frac{\alpha_2 \tan\varphi_0}{l\cos^3\theta_0}t + 3b_1t^2 + 4b_2t^3 + 5b_3t^4\right) \tag{15}$$

$$\ddot{y}(t) = \left(\frac{\alpha_2 \tan\varphi_0}{l\cos^3\theta_0} + 6b_1t + 12b_2t^2 + 20b_3t^3\right) \tag{16}$$

$$\dot{x}(t) = \left(\frac{\left(2T(x_T - x_0) - T\left|x_T - x_0\right| + 2\left|x_T - x_0\right|t\right)}{2T^2}\right) \tag{17}$$

$$\ddot{x}(t) = \left(\frac{\left|x_T - x_0\right|}{T^2}\right) \tag{18}$$

The absolute vehicle velocity can be calculated from equations (15) to (18) with:

$$v_1(t) = \frac{\sqrt{\dot{x}^2 + \dot{y}^2}}{r} \tag{19}$$

$$\dot{\theta} = \frac{\ddot{y}\dot{x} - \ddot{x}\dot{y}}{\dot{x}^2 + \dot{y}^2} = \frac{\tan\varphi}{l} r v_1 \tag{20}$$

Simulation for this flatness technique is conducted with $l = 2m$, $r = 0.25m$, $x(0) = [0,0,0,0]^{'}$, $x(T) = \left[10,10,0,\frac{\pi}{6}\right]^{'}$, and $T = 100$. Figure 2 shows the trajectory and the velocity. Figure 3 shows the vehicle body angle, θ, and the steering angle, φ, corresponding to their angular velocities, $\dot{\theta}$, and, $\dot{\varphi}$.

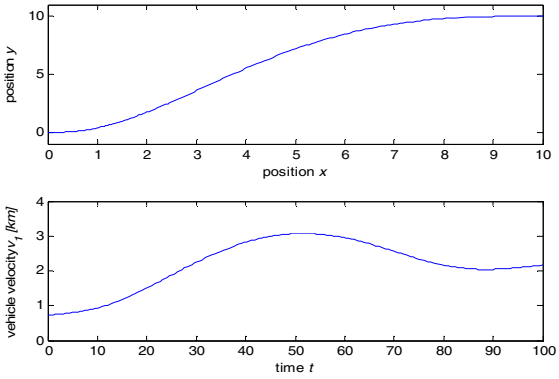

Fig. 2 Trajectory and velocity

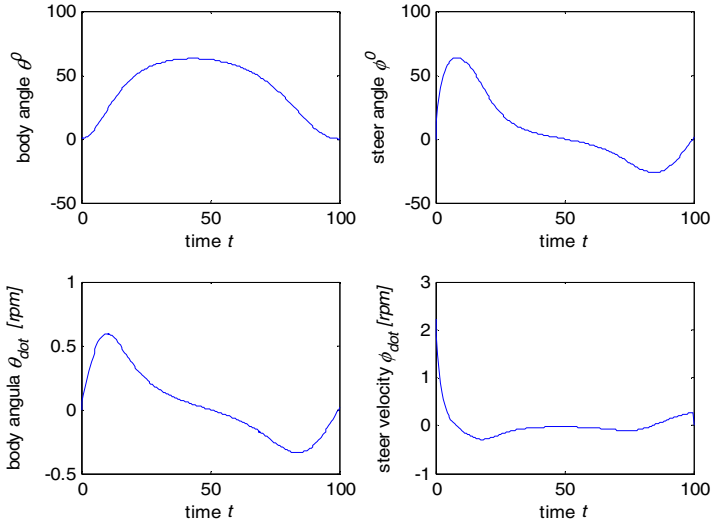

Fig. 3 Body and steering angle

Due to the size of this paper, the sideslip of the vehicle model is ignored. In reality, the sideslip of a vehicle depends on the tire stiffness and the cornering velocity. Then the trajectory generation in this study does not depend on the vehicle velocity. Next part, a new vehicle trajectory generation based on polynomial equations is investigated.

4 Polynomial Trajectory Generations

For faster generation of a feasible vehicle tracking, a second order polynomial for trajectory generation is presented. The equation (1) is separated into the following forms:

$$z_1 = x\,,\ z_2 = \frac{\tan\varphi}{l\cos^3\theta}\,,\ z_3 = \tan\theta\,,\ \text{and}\ \ z_4 = y \tag{21}$$

$$\dot{z}_1 = \dot{x} \tag{22}$$

$$\dot{z}_2 = \frac{v_2 l\cos^2\theta + 3rv_1\cos\theta\sin\theta\sin^2\varphi}{l^2\cos^5\theta\cos^2\varphi} \tag{23}$$

$$\dot{z}_3 = \frac{\tan\varphi}{l\cos^2\theta} rv_1 \tag{24}$$

$$\dot{z}_4 = \dot{y} = \sin\theta rv_1 \tag{25}$$

The vehicle will move from the initial state $(x_0, y_0, \theta_0, \varphi_0)$ at time $t = 0$ to the final state $(x_T, y_T, \theta_T, \varphi_T)$ at time $t = T$ corresponding from the initial state at $(z_{1.0}, z_{2.0}, z_{3.0}, z_{4.0})$ to the final state at $(z_{1.T}, z_{2.T}, z_{3.T}, z_{4.T})$.

For $0 \le t \le T$, the calculation of $[z_1(t), z_2(t), z_3(t), z_4(t)]$ will be:

$$z_1(t) = z_{1.0} + gt \tag{26}$$

$$z_2(t) = z_{2.0} + h_1 t + \frac{1}{2}h_2 t^2 + \frac{1}{3}h_3 t^3 \tag{27}$$

$$z_3(t) = z_{3.0} + gz_{2.0}t + \frac{1}{2}gh_1 t^2 + \frac{1}{6}gh_2 t^3 + \frac{1}{12}gh_3 t^4 \tag{28}$$

$$z_4(t) = z_{4.0} + gz_{3.0}t + \frac{1}{2}g^2 z_{2.0}t^2 + \frac{1}{6}g^2 h_1 t^3 + \frac{1}{24}g^2 h_2 t^4 + \frac{1}{60}g^2 h_3 t^5 \tag{29}$$

with $g = \frac{z_{1.T} - z_{1.0}}{T}$, $[h_1, h_2, h_3]' = D^{-1}e$, $D = \begin{bmatrix} T & \frac{1}{2}T^2 & \frac{1}{3}T^3 \\ \frac{1}{2}gT^2 & \frac{1}{6}gT^3 & \frac{1}{12}gT^4 \\ \frac{1}{6}g^2T^3 & \frac{1}{24}g^2T^4 & \frac{1}{60}g^2T^5 \end{bmatrix}$ and $e = \begin{bmatrix} z_{2.T} - z_{2.0} \\ z_{3.T} - z_{3.0} - gz_{2.0}T \\ z_{4.T} - z_{4.0} - gz_{3.0}T - \frac{1}{2}g^2 z_{2.0}T^2 \end{bmatrix}$.

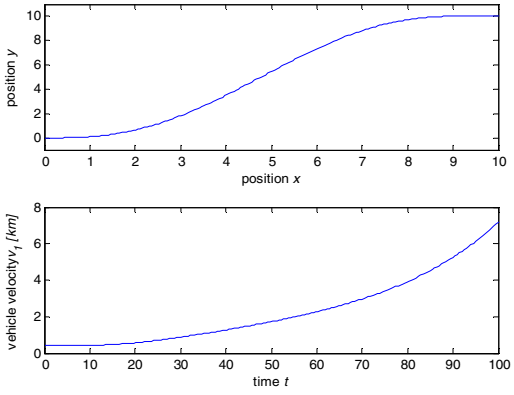

Fig. 4 Trajectory and velocity

Simulation of this method is conducted with the same parameters in section 2 and shown in figure 4 and figure 5.

Figure 4 shows the trajectory for the vehicle from initial point to the final point, and the velocity of the vehicle.

Figure 5 shows the vehicle body angle, θ and the steering angle, φ corresponding to the angular velocity, $\dot{\theta}$ and, $\dot{\varphi}$ of the vehicle.

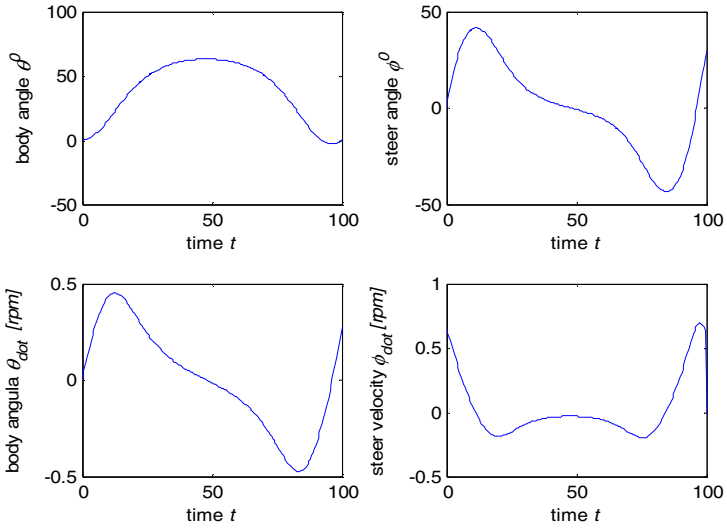

Fig. 5 Body and steering angle

From figure 4, it is really not realistic when the vehicle speed is increasing exponentially. It is expected that, when a vehicle is moving from one point to another point, the speed will increase gradually at the starting point and decrease gradually to the destination point. Therefore in next part, new symmetric polynomial equations in third order are investigated.

5 Symmetric Polynomial Trajectory Generations

Since the system is flatness and each flat output can be parameterized by a sufficiently smooth polynomials. Symmetric third order polynomial equations are tried for this trajectory generation. Because the sideslip is ignored and then, the vehicle trajectory doesn't depend on its speed, v_1, and on the travelling time, T. A new time variable, therefore, for this system is applied with a ratio of $\frac{t}{T}$ for $t = 0 \div T$:

$$x(t) = -(\frac{t}{T} - 1)^3 x_0 + \left(\frac{t}{T}\right)^3 x_T + a_x \left(\frac{t}{T}\right)^2 (\frac{t}{T} - 1) + b_x \frac{t}{T} (\frac{t}{T} - 1)^2 \qquad (30)$$

$$y(t) = -(\frac{t}{T}-1)^3 y_0 + \left(\frac{t}{T}\right)^3 x_T + a_y \left(\frac{t}{T}\right)^2 (\frac{t}{T}-1) + b_y \frac{t}{T}(\frac{t}{T}-1)^2 \quad (31)$$

$$\dot{x}(t) = -3(\frac{t}{T}-1)^2 x_0 + 3\left(\frac{t}{T}\right)^2 x_T + a_x 2\frac{t}{T}(\frac{t}{T}-1) + a_x\left(\frac{t}{T}\right)^2 + b_x(\frac{t}{T}-1)^2 + b_x 2\frac{t}{T}(\frac{t}{T}-1) \quad (32)$$

$$\dot{y}(t) = -3(\frac{t}{T}-1)^2 y_0 + 3\left(\frac{t}{T}\right)^2 y_T + a_y 2\frac{t}{T}(\frac{t}{T}-1) + a_y\left(\frac{t}{T}\right)^2 + b_y(\frac{t}{T}-1)^2 + b_y 2\frac{t}{T}(\frac{t}{T}-1) \quad (33)$$

Then,

$$\ddot{x}(t) = -6(\frac{t}{T}-1)x_0 + 6\frac{t}{T}x_T + a_x 2(2\frac{t}{T}-1) + a_x 2\frac{t}{T} + b_x 2(\frac{t}{T}-1) + b_x 2(2\frac{t}{T}-1) \quad (34)$$

$$\ddot{y}(t) = -6(\frac{t}{T}-1)y_0 + 6\frac{t}{T}y_T + a_y 2(2\frac{t}{T}-1) + a_y 2\frac{t}{T} + b_y 2(\frac{t}{T}-1) + b_y 2(2\frac{t}{T}-1) \quad (35)$$

The constraint on speed:

$$rv_1 = \frac{\dot{x}}{\cos\theta} = \frac{\dot{y}}{\sin\theta} \quad (36)$$

The constraint at starting point $t = 0$:

$$\dot{x}(0) = k_0 \cos\theta_0 \text{ , and } \dot{y}(0) = k_0 \sin\theta_0 \quad (37)$$

The constraint at destination point $t = T$:

$$\dot{x}(T) = k_T \cos\theta_T \text{ , and } \dot{y}(T) = k_T \sin\theta_T \quad (38)$$

From equation (36) and (38), for the calculation simplicity, it is assumed that the speed coefficients at the start and destination point, $k_0 = k_T = k$, then,

$$a_x = k\cos\theta_T - 3x_T \text{ , and } b_x = k\cos\theta_0 - 3x_0 \quad (39)$$

$$a_y = k\sin\theta_T - 3y_T \text{ , and } b_y = k\sin\theta_0 - 3y_0 \quad (40)$$

Simulation is conducted with the same parameters and shown in figure 6 and figure 7.

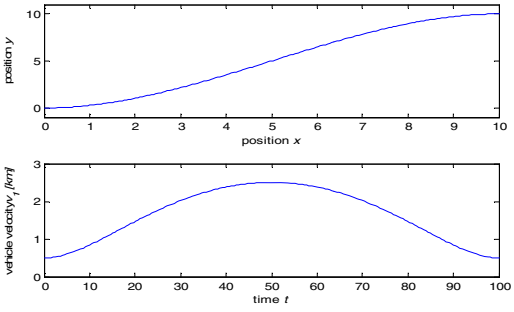

Fig. 6 Trajectory and velocity

It can be seen from figure 6 that the trajectory of this symmetric polynomial is more realistic because the velocity increases from the starting point and decreases in the destination point as per the expectation.

The maximum steering angle for the symmetric polynomial method is $\varphi = 41.1622^0$ and satisfied the constraint, $-45^0 \le \varphi \le 45^0$. This steer angle is smaller than the steer angle in the second order polynomial method.

Comparison performances of the three methods on the trajectory generation and the vehicle velocity are shown in figure 8 and figure 9.

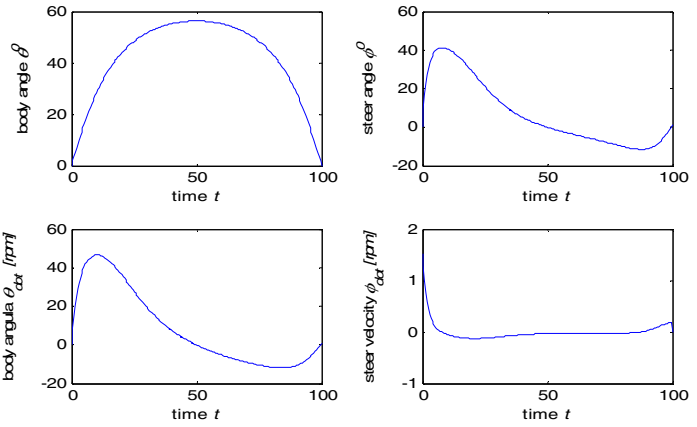

Fig. 7 Body and steering angle

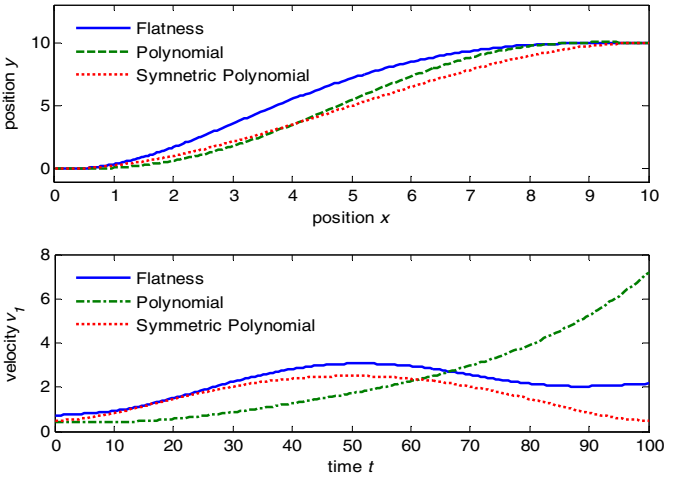

Fig. 8 Comparison of trajectory and velocity

It can be seen that the symmetric polynomial generation can produce a more realistic speed and a smoother trajectory since it allows the vehicle gradually increasing the speed at the start point and reducing the speed to the destination point.

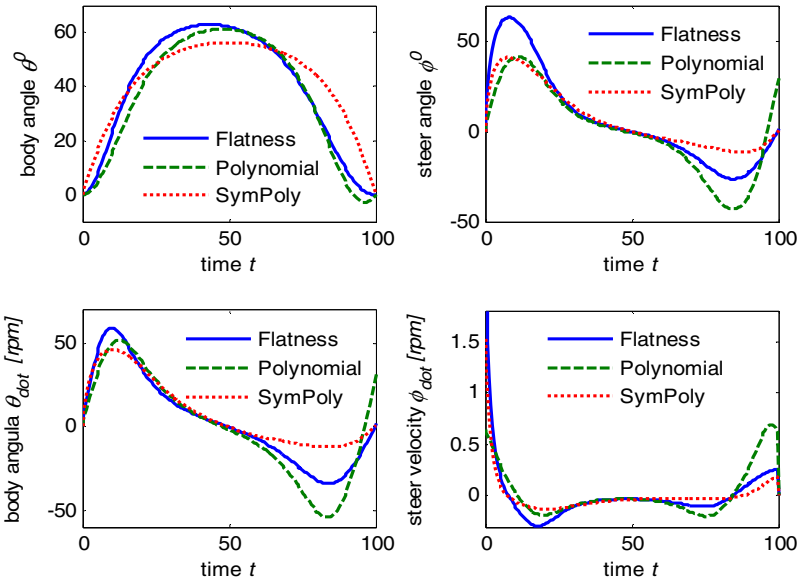

Fig. 9 Comparison of body and steering angle

Figure 9 shows that the symmetric polynomial method providing the lowest body angle, $\theta(t)$, the body angle velocity, $\dot{\theta}(t)$; the steering angle, $\varphi(t)$, and the steering angle velocity, $\dot{\varphi}(t)$. Therefore, this method is recommended for the development of an automatic control of tracking vehicles.

6 Conclusions

The paper has presented three methods of trajectory generation for autonomous vehicles subject to constraints. Regarding to the real vehicle speed development, the third order symmetric polynomial trajectory is recommended. Simulations and analyses are also conducted for vehicle moving in forward and in reverse speeds. Results from this study can be used to develop a real-time control system for auto-driving and auto-parking vehicles. The limitation of this study is the ignorance of the vehicle sideslip due to the cornering velocity. However this error can be eliminated with the feedback control loop and some offset margin of the steer angle constraint.

Acknowledgments. The author would like to thank the Estonian Ministry of Education and Research (Project SF0140113Bs08) for financial support of this study.

References

[1] Levine, J.: Analysis and Control of Nonlinear System, a Flatness-based Approach, 1st edn., pp. 319–328. Springer (2009)
[2] Dong, W., Guo, Y.: New Trajectory Generation for Nonholonomic Mobile Robots. In: Proc. International Symposium on Collaborative Technologies and Systems, pp. 353–358 (2005)
[3] Gomez, M.: Optimal control for Wheeled Mobile Vehicles based on Cell Mapping Techniques. In: Intelligent Vehicles Symposium, pp. 1009–1014 (2008)
[4] Wang, J., Lu, Z., Chen, W., Wu, X.: An Adaptive Trajectory Tracking Control of Wheeled Mobile Robots. In: 6th Proc. on Industrial Electronics and Applications, pp. 1156–1160 (2011)
[5] Werling, M., Kammel, S., Ziegler, J., Groll, L.: Optimal Trajectories for Time-critical Street Scenarios Using Discretized Terminal Manifolds. International Journal of Robotics Research 31(3), 346–359 (2011)
[6] Kanjanawanishkul, K., Hofmeister, M., Zell, A.: Smooth Reference Tracking of a Mobile Robot using Nonlinear Model Predictive Control. In: Proc. of 4th European Conference on Mobile Robots, pp. 161–166 (2009)
[7] Klancar, G.: Tracking-error Model-based Predictive Control for Mobile Robots in real time. Robotics and Autonomous Systems 55(6), 460–469 (2007)
[8] Minh, V.T.: Vehicle Steering Dynamic Calculation and Simulation. In: Proc of 23rd Symp DAAAM International Vienna, pp. 237–242 (2012)
[9] Minh, V.T., Nitin, A.: A Comparative Study on Computational Schemes for Nonlinear Model Predictive Control. Asian Journal of Control 8(4), 324–331 (2006)
[10] Minh, V.T.: Fuzzy logic and slip controller of clutch and vibration for hybrid vehicle. International Journal of Control, Automation and Systems 11(3), 526–532 (2013)